Kinetics of Luminal Proton Binding to the SR Ca-ATPase

Andreas Fibich and Hans-Jürgen Apell*
Department of Biology, University of Konstanz, Konstanz, Germany

ABSTRACT An open membrane preparation containing SR Ca-ATPase was prepared from sarcoplasmic-reticulum vesicles to study the ion binding kinetics in the P-E_2 conformation. Because Ca^{2+} and H^+ binding are electrogenic reactions, fluorescent styryl dyes could be used to determine changes in the binding site occupation in equilibrium titration experiments and time-resolved relaxation processes triggered by a pH jump. By photo release from caged proton the pH of the electrolyte could be decreased in a step of 0.1 pH units by a single ultraviolet-laser flash. Analysis of the pH-jump induced relaxation process in the P-E_2 conformation showed that three Ca-ATPase-specific processes could be identified, fast H^+ binding ($\tau < 100$ μs) and pH-insensitive conformational relaxations after the release of the Ca^{2+} ion (τ ~160 ms), and a slow process (τ ~3.4 s) whose origin could not be unambiguously revealed. The Ca^{2+}-binding affinity in the P-E_2 conformation was reduced with increasing pH, a behavior that can be explained by a reversible transition of the empty P-E_2 state to an inactivated state of the ion pump. All findings are interpreted in the framework of the Post-Albers pump cycle introduced previously, supplemented by an additional transition to an inhibited state of the ion pump.

INTRODUCTION

The Ca-ATPase of the sarcoplasmic reticulum (SR) is an essential enzyme of the locomotor system of animals. Contraction and relaxation of muscle fibers depend on the cytoplasmic calcium concentration. When Ca^{2+} is released through ion channels from the SR, the main storage compartment of Ca^{2+} ions, the muscle fibers contract. The SR Ca-ATPases immediately recycle Ca^{2+} back into the luminal compartment of the SR and thus induce muscle relaxation. To cause muscle relaxation, the cytoplasmic Ca^{2+} concentration has to be reduced from >10 μM to below 0.1 μM in time intervals as short as 50 ms. This powerful uphill transport of Ca^{2+} is mainly performed by the SR Ca^{2+} pumps, which constitute >70% of the proteins in the SR membrane and reach a density in this membrane of ~30,000 μm^{-2} (1). This high density rather than a high pump rate provide the observed high muscle relaxation speed (2). The stoichiometry of the SR Ca-ATPase was determined to be 2 Ca^{2+}/2 H^+/1 ATP (3–5). Due to the high permeability of the SR membrane for cations other than Ca^{2+} the counter transport of H^+ was under debate for quite a while. However, in addition to the experimental proof (4), it was eventually concluded that the stability of the ion-binding sites in the P-E_2 conformation of the protein is maintained by protons bound to the sites in the absence of Ca^{2+} ions (6).

To understand the molecular mechanism of active ion transport by this P-type ATPase, it is extremely helpful that in the meantime the SR Ca-ATPase structure became available in a resolution of a few Angstroms in numerous conformational states of the pump cycle (7–15). Functional details have been known for several decades, and were discussed on the basis of the so-called Post-Albers pump cycle (5,16,17). This cycle describes the transport of two Ca^{2+} from the cytosol to the SR lumen and a counter transport of two protons in a ping-pong mode in which the enzyme becomes phosphorylated in the first half cycle and dephosphorylated in the second half cycle. The enzymatic activity catalyzes the transition between both basic conformations, E_1 and P-E_2, in which the ion-binding sites are accessible from the cytoplasm and the luminal aqueous compartment of the SR, respectively. It has been shown that only the ion binding and release steps in both conformations are electrogenic, i.e., net electric charge is moved into and out of the membrane dielectric (2,18,19). This property has been and still is used to study details of the ion translocation kinetics and the molecular mechanism of the ion transport.

Most of the functional studies were performed with vesicular preparations purified from SR membranes where the cytoplasmic side faces the outside, as in cells. This is a perfect condition to study the interaction of transported ions with their binding sites in E_1, and the interaction of ATP with the enzyme, which is performed with the cytoplasmic domains of the protein (for review see (6)). Studies of luminal ion-binding properties of the Ca-ATPase were performed so far with SR vesicles whose membrane was made permeable for Ca^{2+} by the ionophore A23187 to gain access to the luminal interface (18). In such a condition, however, only equilibrium titration experiments could be performed. Studies of time-resolved kinetics of ion interactions with the binding sites in the P-E_2 conformation were impossible due to a restricted access. For experimental studies under such conditions the effect (or influence) of the (unknown) pH-buffering capacity of the luminal lipid surface would have to be taken into account. Due to the large surface/volume ratio inside the vesicles the concentration of free protons hardly can be controlled. Recently, an

Submitted July 21, 2011, and accepted for publication September 13, 2011.

*Correspondence: h-j.apell@uni-konstanz.de

Editor: Robert Nakamoto.

0006-3495/11/10/1896/9 $2.00

doi: 10.1016/j.bpj.2011.09.014

open microsomal membrane preparation obtained from SR vesicles was introduced, which allows a direct access to the luminal binding sites in the P-E_2 conformation (20). Such membrane preparations were used to perform the following study on partial reactions of the Ca-ATPase induced by luminal H^+ binding.

MATERIALS AND METHODS

Chemicals

Phosphoenolpyruvate, pyruvate kinase, lactate dehydrogenase, NADH, and the Ca^{2+} carrier A23187 were obtained from Boehringer (Mannheim, Germany). The chelator BAPTA (1,2-*bis*(o-aminophenoxy)ethane-*N*,*N*,*N*′,*N*′-tetraacetic acid, 4Na) was obtained from MoBiTec, Göttingen, Germany. Caged proton, 2-methoxy-5-nitrophenylsulfate sodium (MNPS.Na) was synthesized in our lab (21). All other reagents were of the highest grade commercially available. The fluorescent styryl dye 2HITC (1-[4-isothiocyanato-*n*-hexyl]-4-[(p-*N*,*N*-diethyl-amino)styryl]pyridinium bromide) (22) was a gift from Dr. H.-D. Martin, University of Düsseldorf, Düsseldorf, Germany, and the closely related fluorescent styryl dye F52 (1-pentyl-4-[(p-*N*,*N*-diethyl-amino)styryl]pyridinium bromide) with the same spectroscopic properties was synthesized in our group.

SR open membrane preparation

First, Ca-ATPase-containing vesicles were prepared from psoas muscles of rabbits by a slightly modified method of Heilmann and collaborators (23). The Ca-ATPase-specific activity was typically 396 μmol Pi per mg protein and h at 37°C and could be increased up to 1175 μmol Pi per mg protein and h in the presence of the Ca^{2+} ionophore, A23187. This vesicular membrane preparation was purified into open membranes according to (20) by a sodium dodecyl sulfate (SDS) incubation with a protein/detergent ratio of 2.3 mg/ml protein per 1.9 mM SDS, and subsequent dialysis to remove the detergent. Enzyme activity of the open membrane preparation was typically 315 μmol Pi per mg protein and h. Enzyme activity was no longer enhanced by the presence of A23187. It has been shown that formation of the open-membrane preparation does not affect significantly the kinetic properties of the Ca-ATPase (20).

Steady-state fluorescence experiments

Fluorescence measurements in equilibrium-titration experiments were performed to determine the concentration dependence of Ca^{2+} and H^+ binding in both principle conformations, E_1 and P-E_2. A HeNe laser with a wavelength of 543 nm (Laser 2000, Wessling, Germany) was used in a self-constructed setup to excite the fluorescence of the electrochromic dyes 2HITC or F52 as published (20). The temperature in the cuvette (2 ml) was maintained at 20°C by a Peltier thermostat. Because in various experiments the Ca^{2+} chelator BAPTA was used, the actual free Ca^{2+} concentrations were calculated by the program WinMaxC (http://www.stanford.edu/~patton/).

Time-resolved fluorescence experiments

pH jump experiments were performed in a self-constructed setup by ultraviolet (UV) flash-induced proton release from caged proton, MNPS.Na, as described recently (21). The same method was applied before to perform Ca^{2+}-concentration jump experiments with caged calcium (2), and ATP concentration jump experiments with NPE-caged ATP (19). In short, the electrochromic fluorescent dye, F52, was excited by a 543 nm HeNe laser from the top of the setup. A quartz lens was adjusted to widen the laser beam and to illuminate the whole solution homogeneously. The emitted light was collected by an ellipsoidal mirror and reflected into the lower, second focus of the mirror where a photomultiplier was located. An interference filter (589 ± 10 nm) selected the emitted light of the styryl dye before passing the entrance window of a photo multiplier (R928, Hamamatsu Photonics, Hamamatsu City, Japan). The bottom of the cuvette was in contact with a thermostated socket (that also stopped the incident light). The temperature was set at 20°C if not mentioned otherwise. To release protons from their caged precursor an UV-light flash (wavelength 351 nm) was generated by an EMG 100 excimer laser (Lambda Physics, Göttingen, Germany) and directed through a quartz lens into the cuvette. Data output was collected, stored, and analyzed on a computer using an AdLink PCI-9112 data-acquisition board from Imtec, Backnang, Germany. This board works with sample rates up to 100 kHz and a resolution of 12 bit.

RESULTS

Comparison of H^+ binding in the E_1 and P-E_2 conformation

Equilibrium pH titrations were performed with open SR membrane fragments to determine the pK values in both principal conformations of the SR Ca-ATPase. Buffer containing 10 mM NaCl and 200 μM $MgCl_2$, pH 6.5, was equilibrated in a fluorescence cuvette at 20°C. No pH buffer was added to the electrolyte to obtain conditions as used in the pH-jump experiments reported below. The stable fluorescence level obtained after the addition of 400 nM 2HITC and 9 μg/ml Ca-ATPase was used as the reference fluorescence level to which subsequent fluorescence changes were normalized. 10 μM BAPTA and an appropriate amount of $CaCl_2$ were added to obtain a free Ca^{2+} concentration of 0.5 μM. pH titrations were performed by the addition of small aliquots of NaOH up to a pH of 7.7–7.9. The actual pH was determined by a pH microelectrode in parallel in a second cuvette with identical contents. With increasing pH the occupation of the ion-binding sites in the Ca-ATPase was reduced, and the 2HITC fluorescence levels increased correspondingly. The analysis of such an experiment is shown in Fig. 1. The pH dependence of the fluorescence level can be fitted by the Hill function,

$$\frac{F(\mathrm{pH}) - F_0}{F_0} = F_{\max} + \frac{\Delta F}{\left(1 + \left(\frac{10^{-\mathrm{pH}}}{10^{-\mathrm{pK}}}\right)^{-n_H}\right)}, \qquad (1)$$

where $F_{\max}$ is the fluorescence level at saturating high pH, ΔF is the maximal fluorescence change between both pH extremes, pK is the half-saturating pH, and n_H is the Hill coefficient. In the experiment shown in Fig. 1, ΔF has been determined to be 0.40 ± 0.02, the pK was 6.65 ± 0.02, and n_H was 2.5, indicating cooperative binding of >1 H^+.

Corresponding experiments were repeated in the P-E_2 conformation of the Ca-ATPase. This conformation is preferentially stabilized by the addition of 200 μM ATP. Addition of ATP transferred the ion pumps predominantly to

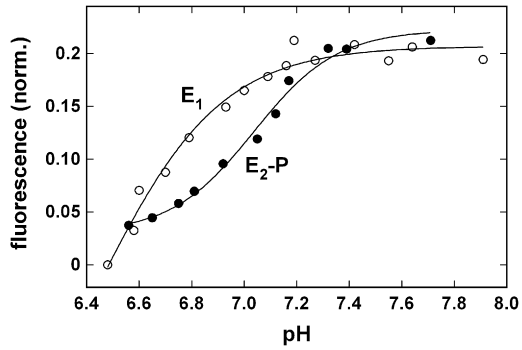

FIGURE 1 Proton binding to the SR Ca-ATPase determined by fluorescence changes of the electrochromic styryl dye 2HITC. pH titrations were performed in the E_1 (*open circles*) and P-E_2 conformation (*solid circles*) of the ion pump. The fluorescence decrease is proportional to the occupation of the ion-binding sites by protons. The concentration dependence has been fitted by the Hill function (Eq.1) with pK values of 6.65 (E_1) and 7.04 (P-E_2). Hill coefficients of >2 indicate cooperative binding of protons.

the P-E_2 conformation (18). The retention of the P-E_2 conformation in this buffer condition has been checked by the tryptic digestion pattern in SDS gel electrophoresis. The analysis of such an experiment is also shown in Fig. 1. Reference level of the fluorescence for normalization was the level before the ATP addition. The fit of the experimental data with Eq. 1 resulted in ΔF of 0.35 ± 0.01, pK = 7.05 ± 0.03, and $n_H = 2.5$. The pK shift of +0.4 compared to the experiment in E_1 indicates a higher proton-binding affinity. The reduced ΔF (~5% smaller) points at higher occupation of the binding sites with H^+ at pH 6.5 in the P-E_2 conformation.

Comparison of Ca^{2+} binding in the E_1 and P-E_2 conformation

In a similar way the Ca^{2+}-binding affinity was determined. Equilibrium titration experiments were performed in buffer containing 25 mM MOPS ((3-(*n*-morpholino)propanesulfonic acid), 50 mM KCl, 1 mM $MgCl_2$, 200 mM choline chloride, 400 μM BAPTA, 400 nM 2HITC, and 9 μg/ml open membrane fragments. pH was adjusted between 6.2 and 7.4 by the addition of appropriate amounts of KOH. When Ca^{2+} binding was studied in the P-E_2 conformation 200 μM ATP were added before the Ca^{2+} titration was performed (18). The amount of $CaCl_2$ added to obtain the desired free Ca^{2+} concentrations was determined in advance by the WinMaxC program. Typical experiments in both conformations, E_1 and P-E_2, at pH 7.2 are shown in Fig. 2 *A*. The fluorescence has been normalized with respect to the fluorescence level in the (nominal) absence of free Ca^{2+}. The concentration dependence could be fitted by the Hill function. The half-saturating Ca^{2+} concentrations, K_D, were 0.38 μM (E_1) and 1.33 μM (P-E_2), the Hill coefficient was 1.0 ± 0.1 in both cases, and the maximal fluorescence

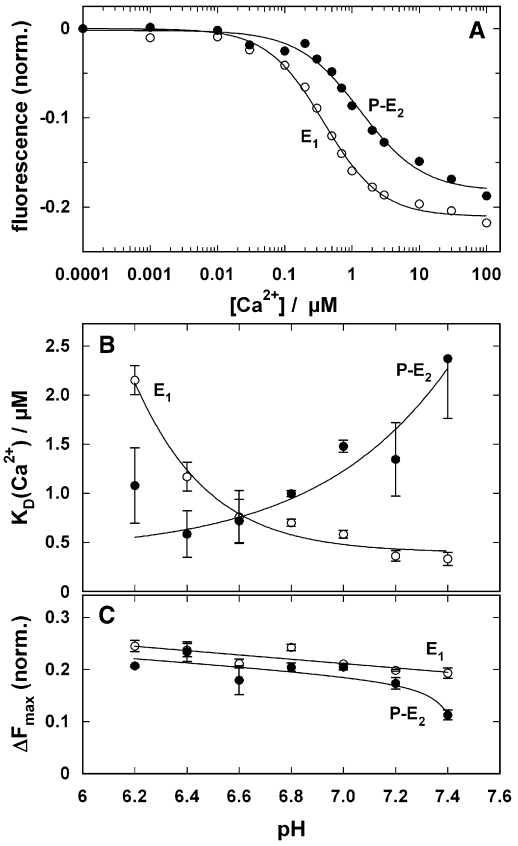

FIGURE 2 Ca^{2+} binding to the SR Ca-ATPase determined by fluorescence changes of the electrochromic styryl dye 2HITC in the E_1 (*open circles*) and P-E_2 conformation (*solid circles*). (*A*) Evaluation of Ca^{2+}-titration experiments with $CaCl_2$ at pH 7.2. The concentration dependence has been fitted by Michaelis-Menten type binding isotherm, $F([Ca^{2+}]) = \Delta F_{max} \cdot [Ca^{2+}]/(K_D + [Ca^{2+}])$, with half-saturating Ca^{2+} concentrations, K_D, of 0.31 μM (E_1) and 1.3 μM (P-E_2). The maximum fluorescence changes, ΔF_{max}, were –21% (E_1) and –18% (P-E_2). (*B*) Corresponding Ca^{2+} titrations were performed at various pH, analyzed, and the respective K_D values are plotted against pH. In the E_1 conformation the K_D values decrease with decreasing H^+ concentrations and indicate competition of both cations for the ion-binding sites. In the P-E_2 conformation K_D increased with pH, indicating that at lower H^+ concentration Ca^{2+} binds with an apparent higher affinity. (*C*) The maximum fluorescence changes, ΔF_{max}, were not significantly pH dependent. Between pH 6.2 and 7.2 the fluorescence level decreased by ~10%, and in P-E_2 the fluorescence changes were slightly smaller than in E_1. The lines in panel *B* and *C* are drawn to guide the eye.

change, ΔF_{max}, were 0.21 ± 0.04 (E_1) and 0.18 ± 0.01 (P-E_2). In the presented titration experiments (up to 100 μM Ca^{2+}) only binding of the first Ca^{2+} was detected because the binding affinity for the second Ca^{2+} is in the order of 2.2 mM (24). Similar experiments were performed at various pH, each repeated up to four times to determine average values. The results are plotted in Fig. 2, *B* (K_D) and *C* (ΔF_{max}). The most interesting finding is that the pH dependence of the K_D value develops in an opposite direction in the E_1 and P-E_2 conformation. In E_1 the apparent Ca^{2+} affinity increases in increasing pH, this behavior is in agreement with the

diminution of the competition between Ca^{2+} and H^+ for the same binding sites at high pH. In the P-E_2 conformation the apparent Ca^{2+} affinity decreases by almost a factor of 5 between pH 6.2 and 7.4 (Fig. 2 *B*). This result is counterintuitive and its mechanistic implications have to be discussed in detail (see below).

Kinetics of H^+ binding in the P-E_2 conformation

The open SR membrane fragments allow for the first time, to our knowledge, to study the luminal H^+-binding kinetics without restriction. Relaxation experiments were performed in which pH jumps are generated in the electrolyte by an UV flash-induced H^+ release from its caged precursor, MNPS.Na, in the microsecond time range correspondingly to previous studies in the E_1 conformation (21). Upon a single flash the pH was decreased by ~0.1 pH units, almost independent of the pH in the range between pH 8.5 and 6.6. The electrolyte contained 50 mM KCl, 1 mM $MgCl_2$, 500 μM MgATP, no pH-buffering substance, 50 μM BAPTA, and an adequate amount of $CaCl_2$ to obtain a free Ca^{2+} concentration of 20 μM. In this condition the Ca-ATPase is maintained preferentially in the P-E_2 conformation with ~1 Ca^{2+} ion in the ion-binding sites (18). The fluorescence cuvette filled with 300 μl electrolyte contained in addition 800 μM of the styryl dye F52, 36 μg/ml Ca-ATPase, and 300 μM MNPS.Na.

After thermal equilibration at 19.5°C in the dark, a UV-laser flash was applied to trigger the release of H^+ from MNPS.Na. The relaxation of the ion pumps into a new steady state has been detected by the time course of the F52 fluorescence. In Fig. 3 two typical experiments are shown, one in the absence and one in the presence of caged proton. In Fig. 3 *A* the immediate response to the UV flash is resolved. The intense UV-light flash produced fluorescence artifacts that decayed basically within the first 2–3 ms. The fluorescence data in the absence of caged proton represent these artifacts, which are caused by traces of fluorescent impurities in the electrolyte and in the quartz of the fluorescence cuvette. The time course could be fitted by one or the sum of two exponentials. The predominant component had a time constant of 0.8 ± 0.1 ms, sometimes a second minor component was found with a time constant of ~7 ± 0.4 ms. When the experiment was repeated in the presence of 300 μM MNPS.Na a fluorescence trace was detected that was shifted to a fluorescence level lower than the initial one within <200 μs. As the difference signal of both traces reveals (Fig. 3 *A*) this observation indicates an unresolved, extremely fast fluorescence decrease that represents an electrogenic process induced by the pH jump. According to the mechanism of fluorescent styryl dyes, a fluorescence decrease corresponds to an uptake of positive charge inside the membrane domain of the ion pump. Because the relaxation was induced by a pH jump it is assigned to H^+ binding. Due to the initial fluorescence artifact the time window from the UV flash (at $t = 0$) up to 2.5 ms has been considered as dead time of the setup. The time course of the fluorescence data at times $t < 2.5$ ms may not to be assigned reliably to the kinetics of Ca-ATPase-dependent processes. In Fig. 3 *B* the time course of the fluorescence signals in the absence and presence of the caged proton, as well as the difference between both signals is shown on a logarithmic t axis for the time period after the dead time until 8 s. Again, the initial, unresolved fluorescence drop (~6%) can be seen, which is followed by a minor but significant fluorescence increase (20 ms < t < 300 ms), and a subsequent small fluorescence decrease (t > 300 ms). The time course of the experiment with caged

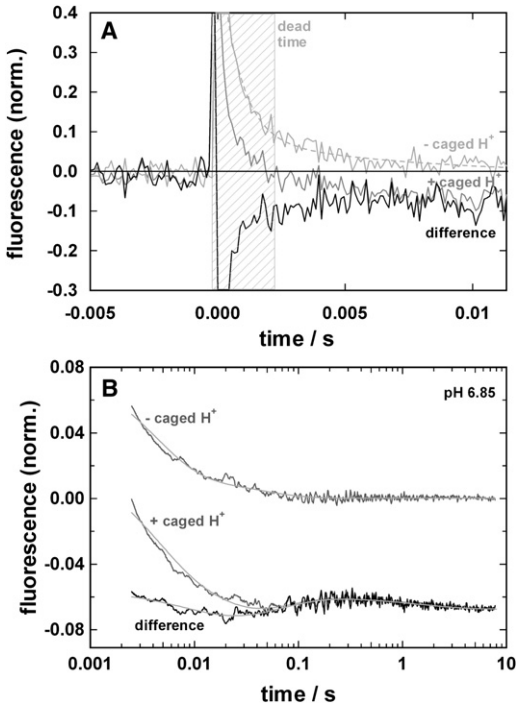

FIGURE 3 pH-jump-induced fluorescence changes on the SR Ca-ATPase in the P-E_2 conformation detected by the styryl dye F52. The pH decrease to pH 6.85 was induced by a release H^+ from its caged precursor, MNPS.Na (caged H^+). The fluorescence amplitude was normalized with respect to the fluorescence level before the proton-releasing UV-laser flash. (*A*) Time course of the fluorescence signals in the absence (*light gray line*) and presence of 300 μM MNPS.Na^+ (*gray line*). The difference of both signals, F(+caged H^+) – F(−caged H^+), is shown in black. As the trace taken without MNPS.Na illustrates, the intense UV flash induced a strong fluorescence artifact that decayed within <5 ms. The difference signal has to be assigned to the interaction of the released protons with the binding sites in the ion pump. Although the time course of the protein-specific process cannot be resolved within the initial time period, the so-called dead time, a significant fluorescence drop had occurred that signifies proton binding to the (*empty*) binding sites. (*B*) Time course of the fluorescence signals (*after the dead time*) between 2.5 ms and ~8 s shown on a logarithmic timescale. The shown traces are averages of two identical experiments. The difference signal reveals a biphasic behavior after the initial fast fluorescence drop. The increase between 20 and 300 ms is caused by a gradual release of positive charge from the binding sites; the subsequent decrease indicates another uptake of positive charge.

H^+ has been fitted by the sum of four exponentials (τ_1 = 3.7 ms, τ_2 = 12.5 ms, τ_3 = 57 ms, τ_4 = 1.8 s), the difference signal with the sum of three exponentials (τ_2 = 11.2 ms, τ_3 = 63 ms, τ_4 = 1.6 s). The agreement between respective time constants, τ_2 to τ_4, obtained from the difference signal and the signal in the presence of caged H^+ was acceptably good. Therefore, we decided to analyze in the following the signals in the presence of caged H^+ without determining each time and in addition the corresponding signal without caged H^+ and calculating the difference signal.

Experiments as shown in Fig. 3 were performed at different pH between pH 6.6 and 8.5 after the pH jump. Two typical fluorescence traces taken at pH 6.9 and 7.9 are shown in Fig. 4 *A*. At pH 6.9 a rising phase in the time window between 30 and 130 ms can be seen, which was absent at pH 7.9. The fluorescence signals have been fitted by a sum of four exponentials, and the respective time constants, τ_i, and fluorescence amplitudes, ΔF_i (i = 1 – 4), are plotted against the electrolyte pH in Fig. 4, *B* and *C*, respectively. At each pH experiments have been repeated two to six times and the average values (mean ± SE) are displayed. The analysis of the time constants, τ_i, obtained from fits yielded the result that none of the monitored reaction steps has a pH-dependent kinetics. Although the electrolyte pH was varied between 6.6 and 8.5 almost by a factor of 100 in H^+ concentration, reasonable average rate constants could be calculated to be τ_1 = 1.25 ± 0.15 ms, τ_2 = 9.4 ± 0.8 ms, τ_3 = 157 ± 30 ms, and τ_4 = 3.4 ± 0.31 s (Fig. 4 *B*). Although the time constant of the fastest process, τ_1, is controlled by the fluorescence artifact, as explained previously, the corresponding fluorescence amplitude, ΔF_1, contains an initial unresolved electrogenic and pump-related process that has to be assigned to H^+ binding. ΔF_1 shows the most prominent pH dependence of all four detected processes (Fig. 4 *C*). Between pH 6.6 and 8.5 the amplitude is reduced by a factor of two. At lower pH obviously more H^+ are bound in the initial fast process upon the pH jump. The second and fourth fluorescence amplitudes belonging to τ_2 and τ_4, respectively, are not significantly pH dependent. They are negative and indicate additional H^+ binding. The fluorescence amplitude ΔF_3 changes its sign at about pH 7.25. At lower pH a fraction of positive charge is released, at higher pH a small amount of positive charge is bound to the Ca-ATPase.

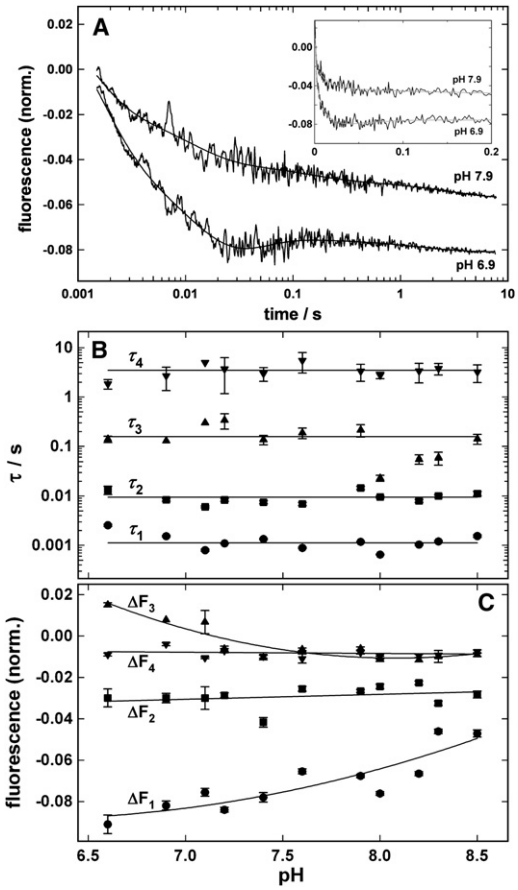

FIGURE 4 pH dependence of the relaxation process upon a pH jump. (*A*) Time course of the F52 fluorescence signal after release of H^+ from caged proton (ΔpH ~ –0.1). The indicated pH was determined after release of H^+. The inset shows the fluorescence signal on a linear timescale, whereas a logarithmic timescale was chosen for the main figure to visualize the complex behavior in a more eye-catching manner. The fluorescence was normalized respective to the level before the H^+-releasing UV flash (t = 0). The time course has been fitted by a sum of four exponentials, $\Delta F_{norm} = \Delta F_1 \cdot \exp(-t/\tau_1) + \Delta F_2 \cdot \exp(-t/\tau_2) + \Delta F_3 \cdot \exp(-t/\tau_3) + \Delta F_4 \cdot \exp(-t/\tau_4)$, as shown by the gray lines. (*B*) pH dependence of the time constants, τ_i, obtained from the fits of the fluorescence experiments as shown in panel *A*. The data points are the averages of 2–6 single experiments, the error bars are mean ± SE. Because no significant pH dependence was obtained the overall averages have been calculated and are shown as horizontal lines through the data. (*C*) pH dependence of the fluorescence amplitudes ΔF_i. The lines drawn through the data are added to guide the eye. ΔF_1 and ΔF_3 show clear pH dependence while ΔF_2 and ΔF_4 are virtually pH independent.

Temperature dependence of H^+ binding in the P-E_2 conformation

pH-jump experiments as shown in Fig. 3 were performed at three different temperatures, 10°C, 20°C, and 30°C (Fig. 5 *A*). The electrolyte used in these experiments contained 50 mM KCl, 1 mM $MgCl_2$, 500 μM MgATP, no pH-buffering substance, 50 μM BAPTA, and an adequate amount of $CaCl_2$ to obtain a free Ca^{2+} concentration of 20 μM. A pH of 6.6 was chosen for these relaxation experiments, the condition in which the transient fluorescence increase and the corresponding time constant, τ_3, were well detectable. To analyze the temperature dependence the time course of the fluorescence signal was fitted as described previously, and the four time constants, τ_i (i = 1 – 4), are displayed as Arrhenius plot (Fig. 5 *B*). The data points (mean ± SE) represented are the average of four individual measurements at each temperature. According to Arrhenius' rate theory, $1/\tau_i = A \cdot \exp(-E_a/RT)$, the slope of the regression line through the data in this semilogarithmic plot is $-E_a/R$, and allows

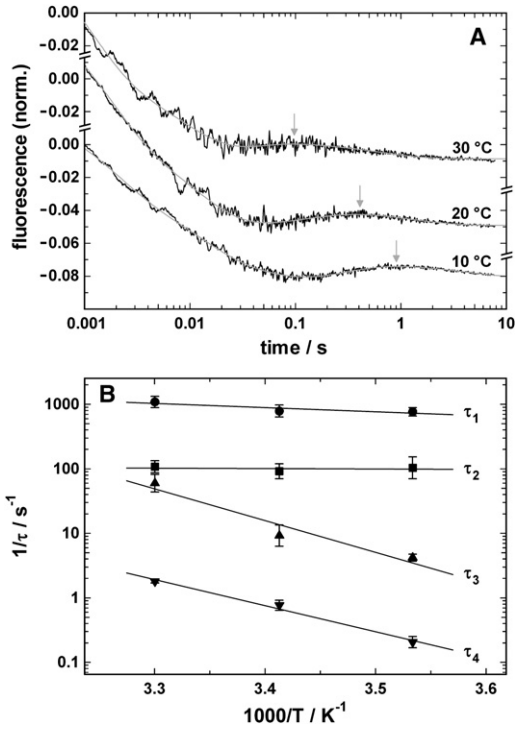

FIGURE 5 Temperature dependence of the relaxation process upon a pH jump. (*A*) Time course of the F52 fluorescence signal at the indicated temperatures in buffer of pH 6.6. The acceleration of the kinetics with temperature can be seen in the reduction of time needed to reach the transient maximum as indicated by the arrows. The time course has been fitted by a sum of four exponentials (as in Fig. 4) and is shown by gray lines. (*B*) The time constants, τ_i, from the fits are represented as Arrhenius plot in which the logarithm of the reciprocal value of τ, which represents a rate constant, is plotted against the reciprocal value of the absolute temperature. In this representation the slope of the regression line through associated data points is proportional to the activation energy of the rate-limiting reaction step: $E_a(\tau_1) = 12.4 \pm 5.3$ kJ/mol, $E_a(\tau_2) = 1.4 \pm 2.0$ kJ/mol, $E_a(\tau_3) = 85.8 \pm 19.0$ kJ/mol, $E_a(\tau_4) = 77.3 \pm 8.0$ kJ/mol.

the determination of the activation energy, E_a. From Fig. 5 *B* it is obvious that the two faster time constants are related to reactions that have a significantly lower activation energy, $E_a(\tau_1) = 12.4 \pm 5.3$ kJ/mol and $E_a(\tau_2) = 1.4 \pm 2.0$ kJ/mol, than the reactions that control the slower time constants, $E_a(\tau_3) = 85.8 \pm 19.0$ kJ/mol and $E_a(\tau_4) = 77.3 \pm 8.0$ kJ/mol. This discrepancy indicates that only the latter two time constants represent enzyme-conformation related reaction steps because the activation energy is >25 kJ/mol, which is required for enzymatic activities.

DISCUSSION

Peinelt and collaborator (18) studied the Ca-ATPase in native SR vesicles and analyzed Ca^{2+} and H^+ binding to the P-E_2 conformation of the ion pump and their competition for the same binding sites. Their experimental handicap was that they had to control luminal pH and Ca^{2+} concentration by equilibrating the ion concentrations across the SR membrane, relying upon ion permeation facilitated by an ionophore. Therefore, it was possible to perform only equilibrium titration experiments. All their experimental results have been interpreted consistently by a branched reaction scheme in the P-E_2 conformation (18):

$$\rightarrow \text{P-E}_2\text{Ca}_2 \leftrightarrow \begin{array}{c}\text{P-E}_2\text{Ca} \\ \updownarrow \\ \text{P-E}_2\text{CaH}\end{array} \leftrightarrow \begin{array}{c}\text{P-E}_2 \\ \updownarrow \\ \text{P-E}_2\text{H}\end{array} \leftrightarrow \text{P-E}_2\text{H}_2 \rightarrow .$$

(Scheme 1)

An important detail of this scheme is the state with mixed occupation of the binding sites, P-E_2CaH, which was inevitable to reproduce their experimental results. The reaction flow through both alternative pathways, P-E_2Ca ↔ P-E_2CaH ↔ P-E_2H and P-E_2Ca ↔ P-E_2 ↔ P-E_2H, is pH controlled in a way that at low pH the first and at high pH the second pathway is preferred. An additional aspect concerning this reaction scheme has to be taken into account. It was deduced from structure-related considerations and may affect this branched pathway: Toyoshima and Inesi (6) have provided evidence that the state with empty binding sites, P-E_2, is unfavorable due to a structural instability of the membrane domain of the SR Ca-ATPase. Therefore, the state P-E_2 may be populated only transiently.

On the basis of our experimental results, the Scheme 1 has to be reconciled with the following specific findings: i), In the P-E_2 conformation the Ca^{2+}-binding affinity increases with pH (Fig. 2 *B*), which is contradictory to the expected behavior and to the findings in the E_1 conformation. ii), All time constants of the relaxation processes upon an applied pH jump are pH independent in the range between pH 6.6 and 8.5 (Fig. 4 *B*). iii), The fastest process has a pH-dependent amplitude, which is reduced with increasing pH by ~50% between pH 6.6 and 8.5 (Fig. 4 *C*). iv), The process characterized by the time constant τ_3 represents below pH 7.25 a release of positive charge and binding of positive charge above pH 7.25 (Fig. 4 *C*). v), The two slow processes, characterized by τ_3 and τ_4, have high activation energies >77 kJ/mol (Fig. 5 *B*), which indicate that the rate-limiting steps in these partial reactions are conformational relaxations of the pump protein rather than ion binding or release steps.

For a detailed analysis one has to keep in mind that in all these experiments 20 μM Ca^{2+} and 500 μM ATP were present, a substrate condition that enables the Ca-ATPase to run continuously through its pump cycle. As has been shown in earlier studies (2), the turnover rate is rather slow at 20°C (<0.8 s^{-1}), and under this condition the rate-limiting step of the cycle is part of the partial reaction that includes proton binding in the P-E_2 conformation. The consequence of this fact is that, before the pH-jump experiment is performed, a steady state in the reaction cycle is maintained in which a major fraction of the pumps resides in the state(s) before the rate-limiting step(s) of the pump

cycle. According to the previously performed study (2), the primarily populated state is P-E_2Ca. When a pH jump is executed the steady state is perturbed, and the relaxation into a new steady state can be monitored by the recorded fluorescence changes as shown in Figs. 3, 4 *A*, and 5 *A*. Because the pH is decreased by ~0.1 units per laser flash, only minor shifts in the steady state are expected, and the observed fluorescence changes in the order of a few percent meet these expectations.

As briefly discussed in the Results section, the time dependence of the fastest protein-related process cannot be resolved due to the fluorescence artifact, which is produced by the setup and parameterized by τ_1. This artifact overlay an obviously extremely fast electrogenic reaction that causes a significant initial fluorescence drop. What can be claimed, however, is a fast initial fluorescence decrease of ~6% that occurred, according to Fig. 3 *A*, within <1 ms, and this process is controlled by an activation energy of 12.4 kJ/mol (or less). Such a behavior is in agreement with the concept that H^+ ions diffuse after their release in the bulk phase through the access channel to the ion-binding sites and are bound there. The electrogenic movement of H^+ in the luminal access channel inside the membrane domain is preferentially diffusion controlled and causes a respectively fast fluorescence decrease after the pH jump. Because the amount of protons released is not significantly pH dependent, it is expected that the fluorescence decrease, ΔF_1, is smaller at pH 8.5 than at pH 6.6 (Fig. 4 *C*) due to the shape of the pH-titration curve that saturates above pH 7.5 (Fig. 1). These findings indicate that the first step of the detected relaxation process is an increased occupation of the ion-binding sites with H^+. According to Scheme 1 this reaction step would be either P-E_2Ca $\rightarrow$ P-E_2CaH or P-E_2 $\rightarrow$ P-E_2H, depending on the pH.

The second exponential of the fit (Fig. 3 *B*) is represented by τ_2 and ΔF_2, both parameters are pH independent (Fig. 4, *B* and *C*), and the associated activation energy is extremely low, $E_a(\tau_2) = 1.4 \pm 2.0$ kJ/mol (Fig. 5). Therefore, we may assume that this fluorescence component is produced by an artifact of the experimental setup, and no Ca-ATPase-related reaction is assigned to this component.

The third component of the fit has pH-dependent fluorescence amplitude, ΔF_3, that changes sign at pH 7.25 (Fig. 4 *C*). ΔF_3 is positive at low pH, which indicates a net release of cations. Looking at Scheme 1, at low pH the ion pumps in the P-E_2 conformation are preferentially distributed between the protonated states P-E_2CaH $\leftrightarrow$ P-E_2H $\leftrightarrow$ P-E_2H_2 in the steady state. Because the experiments were performed in the presence of 20 μM free Ca^{2+} the occupation of the states in this reaction sequence is shifted to the left side, and preferentially contains one Ca^{2+} ion in the binding sites as predicted by the Ca^{2+} titration experiments (Fig. 2 *A*). After the pH jump additional H^+ binding takes place, the steady state is shifted slightly to the right, and overall the Ca^{2+} ion is exchanged against an H^+ in a (small) fraction of pumps. This modification is accompanied by the required net reduction of positive charge in the binding sites, and thus leads to a small fluorescence increase. Because this process has a pH-independent time constant $\tau_3 = 157$ ms and an activation energy of ~85 kJ/mol, it is apparently not controlled by a proton-dependent reaction step but by a (minor) conformational rearrangement in the membrane domain. Comparably high activation energy has been also identified when protons bind to the SR Ca-ATPase in the E_1 conformation (21). It has been shown that in E_1 each H^+ binding step is preceded and followed by a (minor) conformational relaxation with similarly high activation energy (21). Therefore, it can be proposed that also in the P-E_2 conformation the reaction sequence has to be expanded to P-E_2CaH $\leftrightarrow$ P-E_2H $\leftrightarrow$ P-E^*_2H $\leftrightarrow$ P-$E^*_2H_2$, in which the transition from P-E_2H to P-E^*_2H indicates a rate-limiting structural relaxation by which the subsequent H^+ binding to the second site becomes favorable.

At high pH the initial steady state consists predominantly in a population of the state's P-E_2Ca $\leftrightarrow$ P-E_2, with a preferred occupation of the Ca^{2+}-containing state, P-E_2Ca. After the pH jump, protons approach the binding sites from the luminal side, bind to the accessible site, P-E_2Ca $\rightarrow$ P-E_2CaH, the steady state is shifted to the lower level in Scheme 1, and this step induces a new steady state in the reaction sequence, P-E_2CaH $\leftrightarrow$ P-E_2H $\leftrightarrow$ P-E^*_2H $\leftrightarrow$ P-$E^*_2H_2$. This transition is accompanied by an increased net binding of protons, which is reflected in the observed negative ΔF_3.

The last component of the fit has an average time constant of 3.4 ± 0.3 s and a pH-independent, fluorescence decrease (~1%), which indicates a minor additional binding of H^+, and it has an activation energy of 77 kJ/mol. Because ΔF_4 is only -0.9 ± 0.06%, it reflects a rather small average increase of the binding site occupation by protons. The time constant, τ_4, of 3.4 s represents an extremely slow relaxation process. Its pH independence and high activation energy indicates that the rate-limiting step is controlled by another conformational relaxation. In the case of a single rate-limiting relaxation process, the time constant, τ, is controlled by the rate constants of the related forward and backward reaction, k_f and k_b, respectively, $\tau = 1/(k_f + k_b)$. This means that the forward rate has to be $<0.3\ s^{-1}$ when τ_4 is 3.4 s. The presented data do not allow an unambiguous assignment to a specific reaction step. However, two reasonable candidates are obvious. The first is the conformation transition back to the E_1 conformation, $E_2(H_2) \rightarrow H_2E_1$ (Fig. 6). This transition has been already identified as an appropriately slow reaction step (21), and it requires high activation energy. When the H^+ concentration is increased by the pH jump the amount of enzyme in state P-E_2H_2 is increased by a small fraction, and the flow through the subsequent reaction sequence, P-E_2H_2 $\rightarrow$ $E_2(H_2)$ $\rightarrow$ H_2E_1, is also slightly enhanced. Because 20 μM Ca^{2+} are

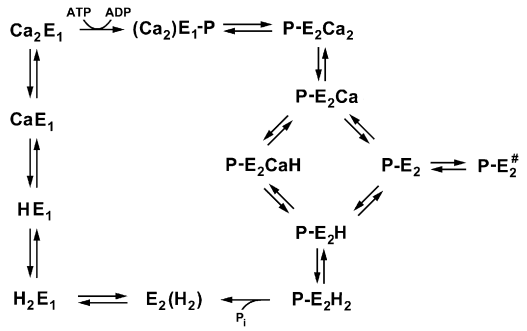

FIGURE 6 Modified Post-Albers scheme of the SR Ca-ATPase. The modification of the reaction pathways were introduced to provide a consistent explanation of the kinetics of the ion binding experiments in the P-E_2 conformation. In the E_1 conformation the scheme is condensed to the states under physiological conditions. In the occluded states, $(Ca_2)E_1$-P and $E_2(H_2)$, access to the binding sites is disabled on both sides of the membrane. The transient state P-E_2 is in a dynamic equilibrium with an inhibited state, P-$E_2^{\#}$.

present, in the E_1 conformation a fast H^+/Ca^{2+} exchange will occur. Overall, the induced slight shift in the steady-state conditions would be controlled by the determined high activation energy and lead, on the average, to a minimal enhancement of positive charge in the binding sites, which is reflected by the fourth component in the fit of the fluorescence trace. A second possible reaction mechanism that could be represented by the τ_4 step will be discussed in the next paragraph.

So far, the results discussed are in agreement with Scheme 1. What cannot be explained by this reaction scheme is, however, the observation that at high pH the Ca^{2+}-binding affinity is decreased (Fig. 2 *B*). Straight forward it is expected that at high pH the competition between Ca^{2+} and H^+ for the same binding sites is lesser than at low pH, and the apparent affinity for Ca^{2+} becomes higher. Such a behavior was observed in the E_1 conformation (Fig. 2 *B*). To explain the reverse behavior an additional constraint has to be introduced. Our suggestion is based on the evidence that empty binding sites in the P-E_2 conformation generate a structural instability (6). When at high pH a noteworthy fraction of the ion pumps reaches the state with empty binding sites, P-E_2, due to the conformational instability this state may be drained considerably into a dead-end state that is unable to bind a Ca^{2+} or H^+, P-E_2 → P-$E_2^{\#}$. This leads to an additional reaction sequence of states at elevated pH, P-E_2Ca ↔ P-E_2 ↔ P-$E_2^{\#}$. When the back reaction rate from the inactivated state, P-$E_2^{\#}$, is small, higher Ca^{2+} concentrations will be required to shift the equilibrium back to the state with bound Ca^{2+} than without the inhibited state. This inhibition mechanism is in our eyes most attractive because it requires only a single modification of the well-established Post-Albers cycle (Fig. 6) to explain the pH dependence of the Ca^{2+} affinity in the P-E_2 conformation, and it is in agreement with structural considerations. This inhibition will be, however, not significant under physiological conditions due to the high Ca^{2+} concentration in the SR. In addition, the presence of the inhibited dead-end state with empty binding sites provides another possibility to explain the slowest relaxation process in the pH-jump experiments. When the states P-E_2Ca ↔ P-E_2 are fractionally drained by H^+ binding after a pH jump, the distribution between both states P-E_2 ↔ P-$E_2^{\#}$ will shift to the left and thus increase the population of pump capable to bind H^+, which in turn decreases the fluorescence level. This reactivating reaction step may be respectively slow and will require a high activation energy since it includes a conformational rearrangement.

In summary, we can state that in the P-E_2 conformation of the SR Ca-ATPase two parallel, pH-controlled reaction sequences are present that describe the Ca^{2+}/H^+ exchange in the ion-binding sites (Fig. 6), as published previously in Scheme 1. In accordance with the observations in the E_1 conformation, rate-limiting conformational relaxations occur after the release of the second Ca^{2+} ion and before binding of the second H^+. When the pumps pass at high pH transiently through the state without ions in the binding site a reversible transition into an inactivated state may take place to which no ions can bind.

The authors thank Milena Roudna for excellent technical assistance, and Dr. Heiko Möller and Anke Friemel for determining the purity of the fluorescence dye F52 by NMR measurements.

This work was financially supported by the Ausschuss für Forschungsfragen of the University of Konstanz, Grant 04/68.

REFERENCES

1. Franzini-Armstrong, C., and D. G. Ferguson. 1985. Density and disposition of Ca^{2+}-ATPase in sarcoplasmic reticulum membrane as determined by shadowing techniques. *Biophys. J.* 48:607–615.
2. Peinelt, C., and H.-J. Apell. 2004. Time-resolved charge movements in the sarcoplasmatic reticulum Ca-ATPase. *Biophys. J.* 86:815–824.
3. de Meis, L. 1985. Role of water in processes of energy transduction: Ca^{2+}-transport ATPase and inorganic pyrophosphatase. *Biochem. Soc. Symp.* 50:97–125.
4. Yu, X., S. Carroll, …, G. Inesi. 1993. H^+ countertransport and electrogenicity of the sarcoplasmic reticulum Ca^{2+} pump in reconstituted proteoliposomes. *Biophys. J.* 64:1232–1242.
5. Yu, X., L. Hao, and G. Inesi. 1994. A pK change of acidic residues contributes to cation countertransport in the Ca-ATPase of sarcoplasmic reticulum. Role of H^+ in $Ca^{(2+)}$-ATPase countertransport. *J. Biol. Chem.* 269:16656–16661.
6. Toyoshima, C., and G. Inesi. 2004. Structural basis of ion pumping by Ca^{2+}-ATPase of the sarcoplasmic reticulum. *Annu. Rev. Biochem.* 73:269–292.
7. Toyoshima, C., M. Nakasako, …, H. Ogawa. 2000. Crystal structure of the calcium pump of sarcoplasmic reticulum at 2.6 A resolution. *Nature.* 405:647–655.
8. Toyoshima, C., and H. Nomura. 2002. Structural changes in the calcium pump accompanying the dissociation of calcium. *Nature.* 418:605–611.
9. Toyoshima, C., H. Nomura, and Y. Sugita. 2003. Crystal structures of Ca^{2+}-ATPase in various physiological states. *Ann. N. Y. Acad. Sci.* 986:1–8.

10. Olesen, C., T. L. Sørensen, …, P. Nissen. 2004. Dephosphorylation of the calcium pump coupled to counterion occlusion. *Science.* 306:2251–2255.

11. Sørensen, T. L., J. V. Møller, and P. Nissen. 2004. Phosphoryl transfer and calcium ion occlusion in the calcium pump. *Science.* 304:1672–1675.

12. Jensen, A. M., T. L. Sørensen, …, P. Nissen. 2006. Modulatory and catalytic modes of ATP binding by the calcium pump. *EMBO J.* 25:2305–2314.

13. Olesen, C., M. Picard, …, P. Nissen. 2007. The structural basis of calcium transport by the calcium pump. *Nature.* 450:1036–1042.

14. Toyoshima, C., Y. Norimatsu, …, H. Ogawa. 2007. How processing of aspartylphosphate is coupled to lumenal gating of the ion pathway in the calcium pump. *Proc. Natl. Acad. Sci. USA.* 104:19831–19836.

15. Laursen, M., M. Bublitz, …, J. P. Morth. 2009. Cyclopiazonic acid is complexed to a divalent metal ion when bound to the sarcoplasmic reticulum Ca2+-ATPase. *J. Biol. Chem.* 284:13513–13518.

16. Inesi, G. 1987. Sequential mechanism of calcium binding and translocation in sarcoplasmic reticulum adenosine triphosphatase. *J. Biol. Chem.* 262:16338–16342.

17. Inesi, G., and L. de Meis. 1989. Regulation of steady state filling in sarcoplasmic reticulum. Roles of back-inhibition, leakage, and slippage of the calcium pump. *J. Biol. Chem.* 264:5929–5936.

18. Peinelt, C., and H.-J. Apell. 2002. Kinetics of the Ca^{2+}, H^{+}, and Mg^{2+} interaction with the ion-binding sites of the SR Ca-ATPase. *Biophys. J.* 82:170–181.

19. Peinelt, C., and H. J. Apell. 2005. Kinetics of Ca^{2+} binding to the SR Ca-ATPase in the E_1 state. *Biophys. J.* 89:2427–2433.

20. Fibich, A., C. Jüngst, and H.-J. Apell. 2008. Properties of the SR Ca-ATPase in an open microsomal membrane preparation. *Open Biochem J.* 2:91–99.

21. Fibich, A., K. Janko, and H. J. Apell. 2007. Kinetics of proton binding to the sarcoplasmic reticulum Ca-ATPase in the E_1 state. *Biophys. J.* 93:3092–3104.

22. Pedersen, M., M. Roudna, …, H. J. Apell. 2002. Detection of charge movements in ion pumps by a family of styryl dyes. *J. Membr. Biol.* 185:221–236.

23. Heilmann, C., D. Brdiczka, …, D. Pette. 1977. ATPase activities, Ca^{2+} transport and phosphoprotein formation in sarcoplasmic reticulum subfractions of fast and slow rabbit muscles. *Eur. J. Biochem.* 81:211–222.

24. Butscher, C., M. Roudna, and H.-J. Apell. 1999. Electrogenic partial reactions of the SR-Ca-ATPase investigated by a fluorescence method. *J. Membr. Biol.* 168:169–181.